

Enhancement of Magnetoresistance Effect in $\text{La}_{0.8-x}\text{Dy}_x\text{Na}_{0.2}\text{MnO}_3$ ($x = 0.00$ and 0.10) Monovalent Doped Manganites: Next Generation Spintronic-Based Devices

*Muhamad Hazim Syakir Bin Suffian, Alif Zaquan Mohd Zi, Nur Amirah Zahrin
Norazila Binti Ibrahim**

*Faculty of Applied Sciences, Universiti Teknologi MARA, 40450, Shah Alam
Selangor, Malaysia*

**Corresponding author; email:noraz954@uitm.edu.my*

Received: 28 August 2024 / Accepted: 18 November 2024

ABSTRACT

$\text{La}_{0.8-x}\text{Dy}_x\text{Na}_{0.2}\text{MnO}_3$ ($x=0.00$ and 0.10) samples were prepared by the solid-state reaction method to investigate the effect of Dy substitution at the La-site on magnetoresistive behaviour in monovalent doped manganites. Analysis of X-ray diffraction data using Rietveld refinement analysis shows that the cell volume decreased from 404.24 \AA^3 to 401.73 \AA^3 indicating the enhancement of lattice distortion as a result of Dy substitution. The resistivity versus temperature, ρ - T curve shows that the $x=0.00$ sample exhibits metallic behaviour in the temperature range of 30 K to 300 K. However, the $x=0.10$ sample exhibit metal-insulator transition, T_{MI} at 220 K. In the presence of 0.8 T of magnetic field, both samples exhibit a reduction in resistivity in the temperature range of 30 K to 300 K which led to magnetoresistance effect. The observed reduction of resistivity indicates an improvement in ferromagnetic interaction between Mn ions, thus conduction process of charge carriers increased. Dy substituted sample exhibit larger magnetoresistance (MR) effect with a value of 48% compared to the $x=0.00$ sample with a value of 10% at 300 K, indicating a high sensitivity of the sample to the magnetic field and its potential application for spintronic-based devices.

Keywords: Dy substitution; manganite; magnetoresistance

INTRODUCTION

The emergence of spintronic technology is based on applying electron spin manipulation to sense magnetic fields and is related to the magnetoresistance (MR) effect [1,2]. The observation of MR effect in manganites, which is attributed to the improvement in spin alignment between Mn ions leads to a decrement in resistivity in the presence of an external magnetic field, indicates the spintronic capability of manganite materials which offers great opportunities for application in new electronic devices for magnetic sensing and magnetic recording [3,4]. Generally, it was reported that manganite material shows a large MR effect at the metal-insulator transition temperature, T_{MI} , however, the value of MR is small for the practical application and the observed maximum MR effect which occurred in a small temperature range at the

vicinity of T_{MI} indicates low stability to the magnetic field of the material in wide temperature range [5].

Interestingly, $\text{La}_{1-x}\text{Na}_x\text{MnO}_3$ for $x = 0.20$ (LN20) exhibits a larger MR effect of 80 % compared with the $x = 0.15$ sample (LN15) which only shows 15 % of the MR value under 1 T magnetic field at 300 K [6] which indicates its potential to be used as magnetic sensor devices. At 300 K, based on the ρ vs T curve, LN20 shows a higher resistivity value compared with LN15. Intriguingly, LN20 also exhibits insulating behaviour while LN15 exhibits metallic behaviour at 300 K. In this case, the enhanced MR effect in the LN20 sample may be related to its insulating behaviour. However, the effect is not fully understood hence a detailed investigation is needed. Therefore, this study is important to elucidate the possible factor that may play an important role as a contributor factor to the enhancement of the MR effect.

Interestingly, it was reported that the MR effect was enhanced by Dy substitution such as in $\text{La}_{0.7-x}\text{Dy}_x\text{Sr}_{0.3}\text{MnO}_3$ as compared to other types of substitution such as in $\text{La}_{0.7-x}\text{Sm}_x\text{Sr}_{0.3}\text{MnO}_3$ and $\text{La}_{0.7-x}\text{Gd}_x\text{Sr}_{0.3}\text{MnO}_3$ [7]. Among these, the highest value of MR maximum was observed at the vicinity of the metal-insulator transition temperature, T_{MI} in Dy substituted samples which is = 620 % while the MR values for both Sm-substituted sample and Gd substituted samples are 175 % and 160 %, respectively. On the other hand, the smallest T_{MI} value in Dy-substituted samples compared to Sm and Gd-substituted samples indicates a weakening of the DE mechanism and enhanced insulating behaviour as a result of Dy substitution [7]. The observed enhancement of MR was suggested due to the enhancement of random magnetic potential and the Coulomb potential induced by extra magnetism of Dy ions [8] which gets suppressed under the presence of the magnetic field. Therefore, substitution of Dy in $\text{La}_{0.8-x}\text{Dy}_x\text{Na}_{0.2}\text{MnO}_3$ may influence the MR-related mechanism and enhance the MR effect. However, there is no report on the effect of magnetic ions substitution on the MR effect in $\text{La}_{0.8-x}\text{Dy}_x\text{Na}_{0.2}\text{MnO}_3$ hence further study is needed. It is also expected that this study will produce a new type of magnetic sensor element with high sensitivity to the magnetic field and can be considered as the next generation of magnetic sensor elements.

MATERIALS AND METHODS

Polycrystalline samples of $\text{La}_{0.8-x}\text{Dy}_x\text{Na}_{0.2}\text{MnO}_3$ ($x = 0.00$ and 0.10) were synthesized via the conventional solid-state method. The starting powders (La_2O_3 , Dy_2O_3 , and MnO_2) with a purity of 99.99% were weighed according to the stoichiometric ratio and thoroughly mixed in an agate mortar for the grinding process for 2 h. The fine powders were then calcined for 24 h at 950 °C in air and reground for another 2 h. Afterward, the powders were pressed into a pellet with a diameter of 13 mm and 5 tons (49 kPa) pressure was applied. The first sintering process was done at 1050 °C for 48 h. The pellets were crushed, reground for 2 h, and pelletized before final sintering at 1150 °C for 72 h. In the present study, the compounds were fully ground in agate and mortar during the grinding process. After each calcination and sintering process, the cooling rate was set at 1 °C/min until it slowly reached room temperature to recover the oxygen lost at a high temperature. The crystal structure of the sample was determined by X-ray diffraction (XRD) via PANanalytical model Xpert PRO that was recorded using Cu K_α ($\lambda = 1.5406 \text{ \AA}$) radiation at room temperature. The data for XRD analysis were collected in the range of $2\theta = 20^\circ - 80^\circ$ with a step size of 0.017° . Rietveld structural refinement was carried out using the GSAS-EXPGUI software. The electrical properties were determined using the standard four-point-probe method in a Janis

model CCS-900T/204 cryostat with He-gas contact at a temperature ranging between 30 and 300 K with an applied current of 5 mA.

RESULTS AND DISCUSSION

Structural Analysis

Figure 1 shows the XRD patterns observed for the $\text{La}_{0.8-x}\text{Dy}_x\text{Na}_{0.2}\text{MnO}_3$ ($x=0.00$ and $x=0.10$) samples in the range of 2θ from 20° to 80° at 300 K. From Figure 1, it is found that the XRD pattern for both samples are the same which indicates the formation of single phased and the absence of impurity phase. The observed diffraction pattern is also found to be similar as reported by Kansara et al. for the $\text{La}_{0.8}\text{Na}_{0.2}\text{MnO}_3$ sample [6].

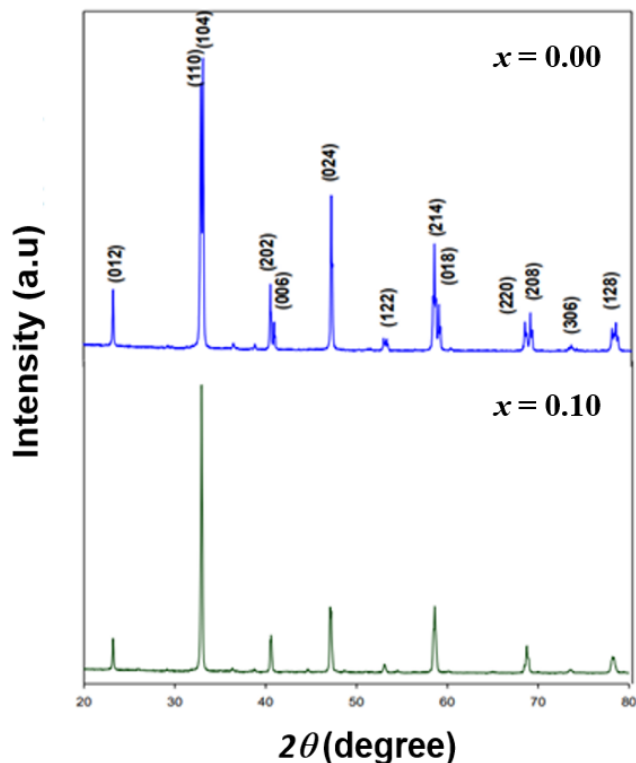


Figure 1. XRD patterns observed for the $\text{La}_{0.8-x}\text{Dy}_x\text{Na}_{0.2}\text{MnO}_3$ ($x=0.00$ and $x=0.10$) samples in the range of 2θ from 20° to 80° at 300 K

Figures 2(a) and 2(b) show the diffraction patterns from the experimental and Rietveld analysis. The black and the red lines reflect experimental data and theoretical data of the sample, respectively, while the blue line at the bottom of both lines represents the differences between both experimental and calculated values which indicates the fitting quality of the analysis. Further, as shown in Table 1 the low value of χ^2 for both samples (1.89 for $x=0.00$ and 2.78 for $x=0.10$) indicated the good quality of refined analysis. The analysis based on the Rietveld refinement technique shows that the samples are crystalline in a rhombohedral unit cell having an $R\bar{3}C$ space group. Table 1 shows the values of the calculated lattice parameters and unit cell volume for both samples obtained from refinement analysis. The obtained lattice parameters for the $x=0.00$ sample found are almost similar as reported by Kansara et al. [6]. As can be seen from

Table 1, Dy substitution reduced the unit cell volume due to its smaller ionic radius [7–9] of 0.107 nm compared to La (0.122 nm) [7].

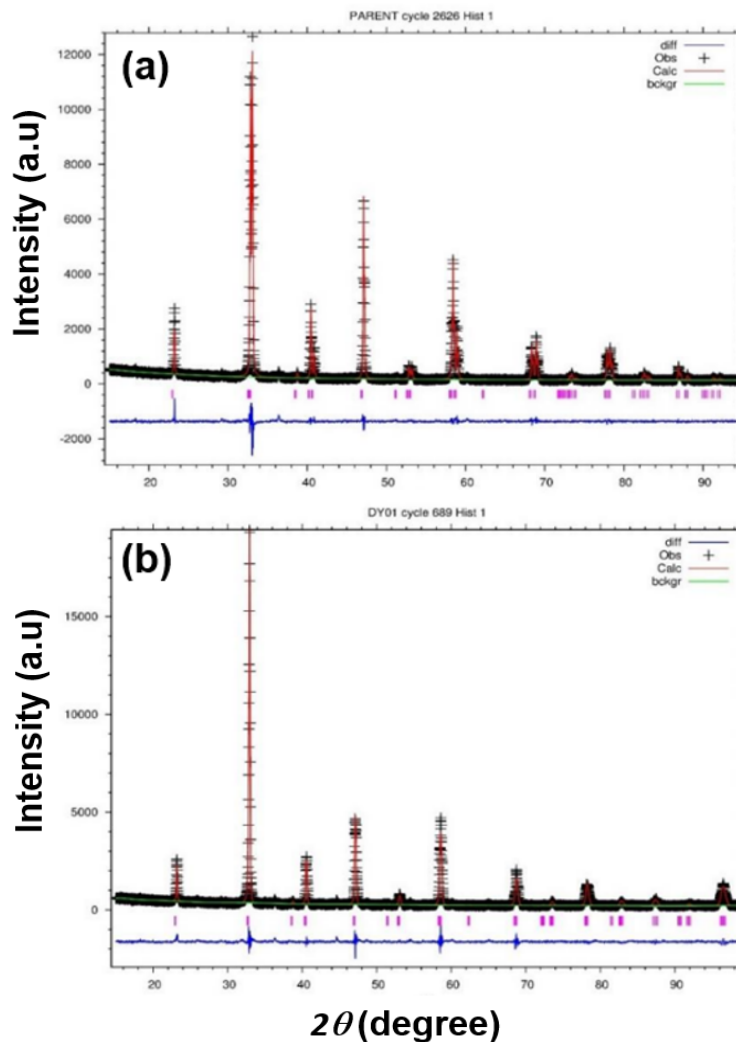


Figure. 2. Diffraction pattern from the experimental and Rietveld analysis for sample (a) $x = 0.00$ and (b) $x = 0.10$. The black and the red lines reflects the experimental data and theoretical data of the sample, respectively, while the blue line at the bottom of both lines represents the differences between both experimental and calculated values.

Table 1. Calculated lattice parameters a , b and c obtained by Rietveld refinements, unit cell volume V and goodness of fit, χ^2

Sample, x	0.00	0.10
Lattice Parameters		
$a/\text{\AA}$	5.5057	5.4793
$b/\text{\AA}$	5.5057	5.4793
$c/\text{\AA}$	13.336	13.381
$V/\text{\AA}^3$	404.24	401.73
χ^2	1.89	2.78

Electrical Properties

Figures 3(a) and 3(b) represent the resistivity versus temperature, ρ - T curves under 0 T and 0.8 T applied magnetic field and 5 mA of applied current for both samples. It can be seen that the $x=0.00$ sample exhibits metallic behaviour in the whole temperature region, while the $x = 0.10$ sample exhibits metal-insulator transition behaviour at the metal-insulator temperature, $T_{MI} = 220$ K. The observed metallic behaviour in the temperature region below T_{MI} is related to the double-exchange (DE) mechanism involving the conduction of itinerant electrons hopping between Mn^{3+} to Mn^{4+} via O^2 . Therefore, the observed temperature dependence of resistivity behaviour for $x = 0.10$ sample indicates that Dy substitution weakened the conduction process of itinerant electrons, hence weakening the double exchange (DE) mechanism in the metallic region. Meanwhile, the observed insulating behaviour above T_{MI} indicates that Dy enhanced the electron-lattice attraction thus leading to the localization of the charge carriers. It is also observed that in the absence of a magnetic field, Dy increased the resistivity in the whole temperature region from 30 K to 300 K. In addition, both samples exhibit a reduction in resistivity with $x = 0.10$ sample exhibit a larger reduction of resistivity under the presence of same strength of the magnetic field of 0.8 T, hence implying that the sensitivity to the magnetic field of the $x=0.10$ sample is larger than that of $x=0.00$ sample. The observed reduction of resistivity in the presence of a magnetic field of 0.8 T for both samples indicates the enhancement of the conduction process of conduction electrons which may be related to the improvement of spin alignment between Mn ions, thus DE is enhanced. It was reported that Dy substitution induced magnetic inhomogeneity due to its extra magnetism and lead to a scattering effect which was further reduced in presence of a magnetic field [7]. Therefore, this could be the reason for the larger drop of resistivity in the Dy substituted sample compared to $x=0.00$ in the present study.

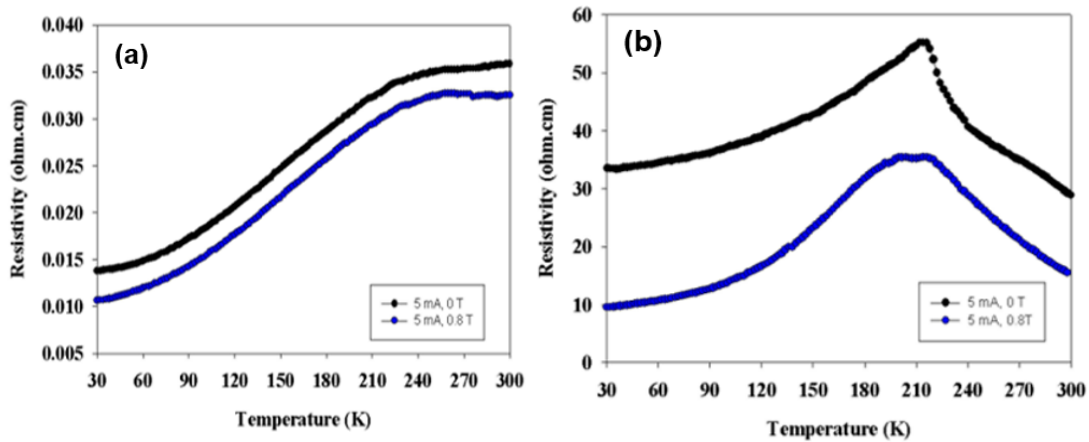


Figure 3. ρ - T curves under 0 T and 0.8 T applied magnetic field and 5 mA of applied current for samples (a) $x = 0.00$ and (b) $x = 0.10$

Magnetoresistance effect

Figure 4 represents the MR vs T plots from 30 to 300 K for $La_{0.8-x}Dy_xNa_{0.2}MnO_3$ ($x = 0.00$ and $x = 0.10$) samples. The MR value has been calculated using the formula $MR (\%) = [(\rho_o - \rho_H)/\rho_o] \times 100$ with ρ_H and ρ_o representing the resistivity of the sample under 0.8 T and 0 T, respectively [7]. As seen from Figure 5, the $x=0.00$ sample exhibit a smaller percentage of MR compared to the $x = 0.10$ sample in the whole measured

temperature region. In comparison, at 30 K the percentage of MR is 25% for the $x=0.00$ sample and 70% for the $x=0.10$ sample. While at 300 K, although both samples exhibit smaller MR value as compared to 30 K, however, Dy substituted sample exhibits a larger MR effect with a value of 48% while for the $x=0.00$ sample, the MR value is 10%. It is possible that the random distribution of Dy may enhance the presence of magnetic inhomogeneity [7,10] in both metallic and insulating regions. In the metallic region, the substitution may interrupt the long-range order of ferromagnetic (FM) interaction between Mn^{3+} -O- Mn^{4+} and induce the formation of Mn^{3+} -O- Mn^{4+} clusters [7]. Further, the substitution may also enhance the antiferromagnetic (AFM) interaction between Mn ions which may arise due to the enhancement of lattice distortion effect as a result of decreased of unit cell volume thus leading to the formation of mixed phases consisting of major FM phase with minor AFM phase. While in the insulating region, the magnetic inhomogeneity may be in the form of FM clusters in the paramagnetic region [10]. In both regions, the presence of a magnetic field improved the spin alignment between Mn ions which may suppress such a mixed phase and lead to the enhancement of FM interaction, hence increasing the conduction process of charge carriers and reduction of resistivity. The finding is interesting which suggests that the presence of magnetic inhomogeneity induced by Dy substitution is an important contributor factor for the enhancement of the MR effect in the $La_{0.8-x}Dy_xNa_{0.2}MnO_3$ ($x=0.10$) sample.

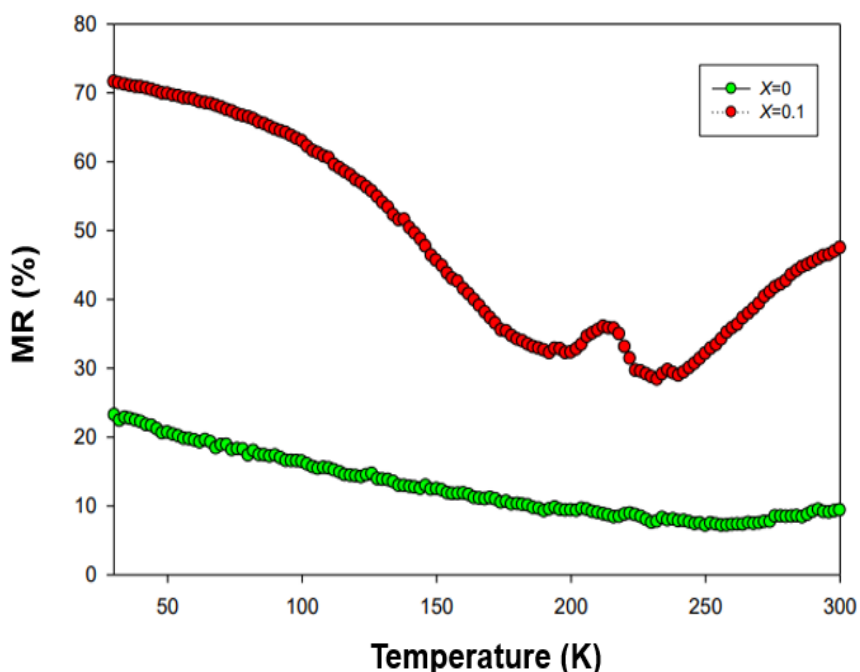


Figure. 4. MR vs T plots from 30 to 300 K for $La_{0.8-x}Dy_xNa_{0.2}MnO_3$ ($x=0.00$ and $x=0.10$) samples

CONCLUSIONS

Studies on the magnetoresistive effect in $La_{0.8-x}Dy_xNa_{0.2}MnO_3$ ($x=0.00$ and $x=0.10$) samples prepared by the solid state method have been discussed in terms of lattice distortion effect and the presence of magnetic inhomogeneity as a result of Dy

substitution. Rietveld analysis of $\text{La}_{0.8-x}\text{Dy}_x\text{Na}_{0.2}\text{MnO}_3$ ($x = 0.00$ and $x = 0.10$) revealed single phase nature of both samples with a decrease in the unit cell volume from 404.24 Å ($x = 0.00$) to 401.73 Å ($x = 0.10$) which indicates that Dy substitution enhanced the lattice distortion effect. Resistivity studies show the metallic behaviour of the $x = 0.00$ sample is transformed to metal-insulator behaviour with an increase in resistivity, indicating that the Dy substitution weakened the double exchange mechanism involving $\text{Mn}^{3+}\text{-O-Mn}^{4+}$ network. A large MR effect has been observed in the whole temperature range for the $x = 0.10$ sample and has been discussed in terms of the presence of magnetic inhomogeneity induced by Dy substitution. According to the large MR effect observed in the $x = 0.10$ sample, the sample could be a suitable material for spintronic-based devices.

ACKNOWLEDGMENTS

The authors would like to thank the Ministry of Higher Education (MOHE), Malaysia, and Universiti Teknologi MARA for supporting this project under the Fundamental Research Grant Scheme (FRGS) [Ref: 600-IRMI/FRGS 5/3 (330/2019)].

REFERENCES

- [1] S. Yang, J. Zhang (2021). Current progress of magnetoresistance sensors, *Chemosensors* **9**, 211.
- [2] M. Pinarbasi, A. Kent (2022). Perspectives on spintronics technology development: Giant magnetoresistance to spin transfer torque magnetic random access memory, *APL Materials* **10**, 020921.
- [3] R. Lukose, N. Zurauskiene, S. Balevicius, V. Stankevic, S. Keršulis, V. Plausinaitiene, R. Navickas (2019). Hybrid graphene-manganite thin film structure for magnetoresistive sensor application, *Nanotechnology* **30**, 355503.
- [4] R. Lukose, N. Zurauskiene, V. Stankevic, M. Vagner, V. Plausinaitiene, G. Niaura, S. Kersulis, S. Balevicius, E. Bolli, and A. Mezzi (2019). Room temperature Co-doped manganite/graphene sensor operating at high pulsed magnetic fields, *Scientific Reports* **9**, 9497.
- [5] N. Zurauskiene, V. Stankevic, S. Kersulis, M. Vagner, V. Plausinaitiene, J. Dobilas, R. Vasiliauskas, M. Skapas, M. Koliada, J. Pietosa (2022). Enhancement of room-temperature low-field magnetoresistance in nanostructured lanthanum manganite films for magnetic sensor applications, *Sensors* **22**, 4004.
- [6] S. Kansara, D. Dhruv, B. Kataria, C. Thaker, S. Rayaprol, C. Prajapat, M. Singh, P. Solanki, D. Kuberkar, and N. Shah (2015). Structural, transport and magnetic properties of monovalent doped $\text{La}_{1-x}\text{Na}_x\text{MnO}_3$ manganites, *Ceramics International* **41**, 7162.
- [7] S. Qixiang, W. Guiying, Y. Guoqing, M. Qiang, W. Wenqi, P. Zhensheng (2008). Influence of the substitution of Sm, Gd, and Dy for La in $\text{La}_{0.7}\text{Sr}_{0.3}\text{MnO}_3$ on its magnetic and electric properties and strengthening effect on room-temperature CMR, *Journal of Rare Earths* **26**, 821.
- [8] N. Ibrahim, A. Yahya (2011). Double metal-insulator peaks and effect of Dy^{3+} substitution on transport and magnetic properties of hole doped $\text{La}_{0.8}\text{Ag}_{0.2}\text{MnO}_3$, *Materials Research Innovations* **15**, s221.

- [9] N. Zaidi, S. Mnefgui, A. Dhahri, J. Dhahri, E. Hlil (2014). The effect of Dy doped on structural, magnetic and magnetocaloric properties of $\text{La}_{0.67-x}\text{Dy}_x\text{Pb}_{0.33}\text{MnO}_3$ ($x= 0.00, 0.15$ and 0.20) compounds, *Physica B: Condensed Matter* **450**, 155.
- [10] I. Sfir, A. Ezaami, W. Cheikhrouhou-Koubaa, A. Cheikhrouhou (2017). Structural, magnetic and magnetocaloric properties in $\text{La}_{0.7-x}\text{Dy}_x\text{Sr}_{0.3}\text{MnO}_3$ manganites ($x= 0.00, 0.01$ and 0.03), *Journal of Alloys and Compounds* **696**, 760.